

# The Random Walk Metropolis: Linking Theory and Practice Through a Case Study

Chris Sherlock, Paul Fearnhead and Gareth O. Roberts

*Abstract.* The random walk Metropolis (RWM) is one of the most common Markov chain Monte Carlo algorithms in practical use today. Its theoretical properties have been extensively explored for certain classes of target, and a number of results with important practical implications have been derived. This article draws together a selection of new and existing key results and concepts and describes their implications. The impact of each new idea on algorithm efficiency is demonstrated for the practical example of the Markov modulated Poisson process (MMPP). A reparameterization of the MMPP which leads to a highly efficient RWM-within-Gibbs algorithm in certain circumstances is also presented.

*Key words and phrases:* Random walk Metropolis, Metropolis–Hastings, MCMC, adaptive MCMC, MMPP.

## 1. INTRODUCTION

Markov chain Monte Carlo (MCMC) algorithms provide a framework for sampling from a target random variable with a potentially complicated probability distribution  $\pi(\cdot)$  by generating a Markov chain  $\mathbf{X}^{(1)}, \mathbf{X}^{(2)}, \dots$  with stationary distribution  $\pi(\cdot)$ . The single most widely used subclass of MCMC algorithms is based around the random walk Metropolis (RWM).

Theoretical properties of RWM algorithms for certain special classes of target have been investigated extensively. Reviews of RWM theory have, for example, dealt with optimal scaling and posterior shape (Roberts and Rosenthal, 2001), and convergence (Roberts, 2003). This article does not set out to be a comprehensive review of all theoretical results pertinent to the RWM. Instead the article reviews and develops specific aspects of the theory of RWM efficiency in order to tackle an important and difficult problem: inference

for the Markov modulated Poisson process (MMPP). It includes sections on RWM within Gibbs, hybrid algorithms, and adaptive MCMC, as well as optimal scaling, optimal shaping, and convergence. A strong emphasis is placed on developing an intuitive understanding of the processes behind the theoretical results, and then on using these ideas to improve the implementation. All of the RWM algorithms described in this article are tested against datasets arising from MMPPs. Realized changes in efficiency are then compared with theoretical predictions.

Observed event times of an MMPP arise from a Poisson process whose intensity varies with the state of an unobserved continuous-time Markov chain. The MMPP has been used to model a wide variety of clustered point processes, for example, requests for web pages from users of the World Wide Web (Scott and Smyth, 2003), arrivals of photons from single-molecule fluorescence experiments (Burzykowski, Szubiakowski and Ryden, 2003; Kou, Xie and Liu, 2005), and occurrences of a rare DNA motif along a genome (Fearnhead and Sherlock, 2006).

In common with mixture models and other hidden Markov models, inference for the MMPP is greatly complicated by a lack of knowledge of the hidden data. The likelihood function often possesses many minor

---

*Chris Sherlock is Lecturer, Department of Mathematics and Statistics, Lancaster University, Lancaster, LA1 4YF, UK (e-mail: c.sherlock@lancaster.ac.uk). Paul Fearnhead is Professor, Department of Mathematics and Statistics, Lancaster University, Lancaster, LA1 4YF, UK. Gareth O. Roberts is Professor, Department of Statistics, University of Warwick, Coventry, CV4 7AL, UK.*

modes since the data might be approximately described by a hidden process with fewer states. For this same reason the likelihood often does not approach zero as certain combinations of parameters approach zero and/or infinity and so improper priors lead to improper posteriors (e.g., Sherlock, 2005). Further, as with many hidden data models the likelihood is invariant under permutation of the states, and this “labeling” problem leads to posteriors with several equal modes.

This article focuses on generic concepts and techniques for improving the efficiency of RWM algorithms whatever the statistical model. The MMPP provides a nontrivial testing ground for them. All of the RWM algorithms described in this article are tested against two simulated MMPP datasets with very different characteristics. This allows us to demonstrate the influence on performance of posterior attributes such as shape and orientation near the mode and lightness or heaviness of tails.

Section 2 introduces RWM algorithms and then describes theoretical and practical measures of algorithm efficiency. Next the two main theoretical approaches to determining efficiency are described, and the section ends with a brief overview of the MMPP and a description of the data analyzed in this article. Section 3 introduces a series of concepts which allow potential improvements in the efficiency of a RWM algorithm. The intuition behind each concept is described, followed by theoretical justification and then details of one or more RWM algorithms motivated by the theory. Actual results are described and compared with theoretical predictions in Section 4, and the article is summarized in Section 5.

## 2. BACKGROUND

In this section we introduce the background material on which the remainder of this article draws. We describe the random walk Metropolis algorithm and a variation, the random walk Metropolis-within-Gibbs. Both practical issues and theoretical approaches to algorithm efficiency are then discussed. We conclude with an introduction to the Markov modulated Poisson process and to the datasets used later in the article.

### 2.1 Random Walk Metropolis Algorithms

The *random walk Metropolis* (RWM) updating scheme was first applied by Metropolis et al. (1953) and proceeds as follows. Given a current value of the  $d$ -dimensional Markov chain,  $\mathbf{X}$ , a new value  $\mathbf{X}^*$  is obtained by proposing a jump  $\mathbf{Y}^* := \mathbf{X}^* - \mathbf{X}$  from the

prespecified Lebesgue density

$$(1) \quad \tilde{r}(\mathbf{y}^*; \lambda) := \frac{1}{\lambda^d} r\left(\frac{\mathbf{y}^*}{\lambda}\right),$$

with  $r(\mathbf{y}) = r(-\mathbf{y})$  for all  $\mathbf{y}$ . Here  $\lambda > 0$  governs the overall size of the proposed jump and (see Section 3.1) plays a crucial role in determining the efficiency of any algorithm. The proposal is then accepted or rejected according to acceptance probability

$$(2) \quad \alpha(\mathbf{x}, \mathbf{y}^*) = \min\left(1, \frac{\pi(\mathbf{x} + \mathbf{y}^*)}{\pi(\mathbf{x})}\right).$$

If the proposed value is accepted it becomes the next current value ( $\mathbf{X}' \leftarrow \mathbf{X} + \mathbf{Y}^*$ ); otherwise the current value is left unchanged ( $\mathbf{X}' \leftarrow \mathbf{X}$ ).

An intuitive interpretation of the above formula is that “uphill” proposals (proposals which take the chain closer to a local mode) are always accepted, whereas “downhill” proposals are accepted with probability exactly equal to the relative “heights” of the posterior at the proposed and current values. It is precisely this rejection of some “downhill” proposals which acts to keep the Markov chain in the main posterior mass most of the time.

More formally, denote by  $P(\mathbf{x}, \cdot)$  the transition kernel of the chain, which represents the combined process of proposal and acceptance/rejection leading from one element of the chain ( $\mathbf{x}$ ) to the next. The acceptance probability (2) is chosen so that the chain is reversible at equilibrium with stationary distribution  $\pi(\cdot)$ . Reversibility [that  $\pi(\mathbf{x})P(\mathbf{x}, \mathbf{x}') = \pi(\mathbf{x}')P(\mathbf{x}', \mathbf{x})$ ] is an important property precisely because it is so easy to construct reversible chains which have a prespecified stationary distribution. It is also possible to prove a slightly stronger central limit theorem for reversible (as opposed to nonreversible) geometrically ergodic chains (e.g., Section 2.2.1).

We now describe a generalization of the RWM which acts on a target whose components have been split into  $k$  sub-blocks. In general we write  $\mathbf{X} = (\mathbf{X}_1, \dots, \mathbf{X}_k)$ , where  $\mathbf{X}_i$  is the  $i$ th sub-block of components of the current element of the chain. Starting from value  $\mathbf{X}$ , a single iteration of this algorithm cycles through all of the sub-blocks updating each in turn. It will therefore be convenient to define the shorthand

$$\mathbf{x}_i^{(B)} := \mathbf{x}'_1, \dots, \mathbf{x}'_{i-1}, \mathbf{x}_i, \mathbf{x}_{i+1}, \dots, \mathbf{x}_k,$$

$$\mathbf{x}_i^{(B)*} := \mathbf{x}'_1, \dots, \mathbf{x}'_{i-1}, \mathbf{x}_i + \mathbf{y}_i^*, \mathbf{x}_{i+1}, \dots, \mathbf{x}_k,$$

where  $\mathbf{x}'_j$  is the *updated value* of the  $j$ th sub-block. For the  $i$ th sub-block a jump  $\mathbf{y}_i^*$  is proposed from symmetric density  $\tilde{r}_i(\mathbf{y}; \lambda_i)$  and accepted or rejected according

to acceptance probability  $\pi(\mathbf{x}_i^{(B)*})/\pi(\mathbf{x}_i^{(B)})$ . Since this algorithm is in fact a generalization of both the RWM and the Gibbs sampler (for a description of the Gibbs sampler see, e.g., Gamerman and Lopes, 2006) we follow, for example, Neal and Roberts (2006) and call this the *random walk Metropolis-within-Gibbs* or RWM-within-Gibbs. The most commonly used random walk Metropolis-within-Gibbs algorithm, and also the simplest, is that employed in this article: here all blocks have dimension 1 so that each component of the parameter vector is updated in turn.

As mentioned earlier in this section, the RWM is reversible; but even though each stage of the RWM-within-Gibbs is reversible, the algorithm as a whole is not. Reversible variations include the *random scan* RWM-within-Gibbs, wherein at each iteration a single component is chosen at random and updated conditional on all the other components.

Convergence of the Markov chain to its stationary distribution can be guaranteed for all of the above algorithms under quite general circumstances (e.g., Gilks, Richardson and Spiegelhalter, 1996).

## 2.2 Algorithm Efficiency

Consecutive draws of an MCMC Markov chain are correlated and the sequence of marginal distributions converges to  $\pi(\cdot)$ . Two main (and related) issues arise with regard to the efficiency of MCMC algorithms: convergence and mixing.

**2.2.1 Convergence.** In this article we will be concerned with practical determination of a point at which a chain has converged. The method we employ is simple heuristic examination of the trace plots for the different components of the chain. Note that since the state space is multidimensional it is not sufficient to simply examine a single component. Alternative techniques are discussed in Chapter 7 of the book by Gilks, Richardson and Spiegelhalter (1996).

Theoretical criteria for ensuring convergence (ergodicity) of MCMC Markov chains are examined in detail in Chapters 3 and 4 of the book by Gilks, Richardson and Spiegelhalter (1996) and references therein, and will not be discussed here. We do, however, wish to highlight the concepts of geometric and polynomial ergodicity. A Markov chain with transition kernel  $P$  is *geometrically ergodic* with stationary distribution  $\pi(\cdot)$  if

$$(3) \quad \|P^n(\mathbf{x}, \cdot) - \pi(\cdot)\|_1 \leq M(\mathbf{x})r^n$$

for some positive  $r < 1$  and  $M(\cdot) \geq 0$ ; if  $M(\cdot)$  is bounded above, then the chain is *uniformly ergodic*.

Here  $\|F(\cdot) - G(\cdot)\|_1$  denotes the total variational distance between measures  $F(\cdot)$  and  $G(\cdot)$  (see, e.g., Meyn and Tweedie, 1993), and  $P^n$  is the  $n$ -step transition kernel. Efficiency of a geometrically ergodic algorithm is measured by the geometric rate of convergence,  $r$ , which over a large number of iterations is well approximated by the second largest eigenvalue of the transition kernel [the largest eigenvalue being 1, and corresponding to the stationary distribution  $\pi(\cdot)$ ]. Geometric ergodicity is usually a purely qualitative property since in general the constants  $M(\mathbf{x})$  and  $r$  are not known. Crucially for practical MCMC, however, any *geometrically ergodic reversible Markov chain satisfies a central limit theorem for all functions with finite second moment with respect to  $\pi(\cdot)$* . Thus there is a  $\sigma_f^2 < \infty$  such that

$$(4) \quad n^{1/2}(\hat{f}_n - \mathbb{E}_\pi[f(\mathbf{X})]) \Rightarrow N(0, \sigma_f^2),$$

where  $\Rightarrow$  denotes convergence in distribution. The central limit theorem (4) not only guarantees convergence of the Monte Carlo estimate (5) but also supplies its standard error, which decreases as  $n^{-1/2}$ .

When the second largest eigenvalue is also 1, a Markov chain is termed *polynomially ergodic* if

$$\|P^n(\mathbf{x}, \cdot) - \pi(\cdot)\|_1 \leq M(\mathbf{x})n^{-r}.$$

Clearly polynomial ergodicity is a weaker condition than geometric ergodicity. Central limit theorems for polynomially ergodic MCMC are much more delicate; see the article by Jarner and Roberts (2002) for details.

In this article a chain is referred to as having “reached stationarity” or “converged” when the distribution from which an element is sampled is as close to the stationary distribution as to make no practical difference to any Monte Carlo estimates.

An estimate of the expectation of a given function  $f(X)$ , which is more accurate than a naive Monte Carlo average over all the elements of the chain, is likely to be obtained by discarding the portion of the chain  $\mathbf{X}_0, \dots, \mathbf{X}_m$  up until the point at which it was deemed to have reached stationarity; iterations  $1, \dots, m$  are commonly termed “burn in.” Using only the remaining elements  $\mathbf{X}_{m+1}, \dots, \mathbf{X}_{m+n}$  (with  $m + n = N$ ) our Monte Carlo estimator becomes

$$(5) \quad \hat{f}_n := \frac{1}{n} \sum_{m+1}^{m+n} f(\mathbf{X}_i).$$

Convergence and burn in are not discussed any further here, and for the rest of this section the chain is assumed to have started at stationarity and continued for  $n$  further iterations.

2.2.2 *Practical measures of mixing efficiency.* For a stationary chain,  $\mathbf{X}_0$  is sampled from  $\pi(\cdot)$ , and so for all  $k > 0$  and  $i \geq 0$

$$\text{Cov}[f(\mathbf{X}_k), f(\mathbf{X}_{k+i})] = \text{Cov}[f(\mathbf{X}_0), f(\mathbf{X}_i)].$$

This is the *autocorrelation* at lag  $i$ . Therefore at stationarity, from the definition in (4),

$$\begin{aligned} \sigma_f^2 &:= \lim_{n \rightarrow \infty} n \text{Var}[\hat{f}_n] \\ &= \text{Var}[f(\mathbf{X}_0)] + 2 \sum_{i=1}^{\infty} \text{Cov}[f(\mathbf{X}_0), f(\mathbf{X}_i)] \end{aligned}$$

provided the sum exists (e.g., Geyer, 1992). If elements of the stationary chain were independent, then  $\sigma_f^2$  would simply be  $\text{Var}[f(\mathbf{X}_0)]$  and so a measure of the inefficiency of the Monte Carlo estimate  $\hat{f}_n$  relative to the perfect i.i.d. sample is

$$(6) \quad \frac{\sigma_f^2}{\text{Var}[f(\mathbf{X}_0)]} = 1 + 2 \sum_{i=1}^{\infty} \text{Corr}[f(\mathbf{X}_0), f(\mathbf{X}_i)].$$

This is the *integrated autocorrelation time* (ACT) and represents the effective number of dependent samples that is equivalent to a single independent sample. Alternatively  $n^* = n/\text{ACT}$  may be regarded as the effective equivalent sample size if the elements of the chain had been independent.

To estimate the ACT in practice one might examine the chain from the point at which it is deemed to have converged and estimate the lag- $i$  autocorrelation  $\text{Corr}[f(\mathbf{X}_0), f(\mathbf{X}_i)]$  by

$$(7) \quad \hat{\gamma}_i = \frac{1}{n-i} \sum_{j=1}^{n-i} (f(\mathbf{X}_j) - \hat{f}_n)(f(\mathbf{X}_{j+i}) - \hat{f}_n).$$

Naively, substituting these into (6) gives an estimate of the ACT. However, contributions from all terms with very low theoretical autocorrelation *in a real run* are effectively random noise, and the sum of such terms can dominate the deterministic effect in which we are interested (e.g., Geyer, 1992). For this article we employ the simple solution suggested by Carlin and Louis (2009): the sum (6) is truncated from the first lag,  $l$ , for which the estimated autocorrelation drops below 0.05. This gives the (slightly biased) estimator

$$(8) \quad \text{ACT}_{\text{est}} := 1 + 2 \sum_{i=1}^{l-1} \hat{\gamma}_i.$$

Given the potential for relatively large variance in estimates of integrated ACT howsoever they might be obtained (e.g., Sokal, 1997), this simple estimator should

be adequate for comparing the relative efficiencies of the different algorithms in this article. Geyer (1992) provided a number of more complex window estimators and provided references for regularity conditions under which they are consistent.

A given run will have a different ACT associated with each parameter. An alternative efficiency measure, which is aggregated over all parameters, is provided by the Mean Squared Euclidean Jump Distance (MSEJD)

$$S_{\text{Euc}}^2 := \frac{1}{n-1} \sum_{i=1}^{n-1} \|\mathbf{x}^{(i+1)} - \mathbf{x}^{(i)}\|_2^2.$$

The expectation of this quantity at stationarity is referred to as the Expected Squared Euclidean Jump Distance (ESEJD). Consider a single component of the target with variance  $\sigma_i^2 := \text{Var}[X_i] = \text{Var}[X'_i]$ , and note that  $\mathbb{E}[X'_i - X_i] = 0$ , so

$$\begin{aligned} \mathbb{E}[(X'_i - X_i)^2] &= \text{Var}[X'_i - X_i] \\ &= 2\sigma_i^2(1 - \text{Corr}[X_i, X'_i]). \end{aligned}$$

Thus when the chain is stationary and the posterior variance is finite, maximizing the ESEJD is equivalent to minimizing a weighted sum of the lag-1 autocorrelations.

If the target has finite second moments and is roughly elliptical in shape with (known) covariance matrix  $\Sigma$ , then an alternative measure of efficiency is the Mean Squared Jump Distance (MSJD)

$$S_d^2 := \frac{1}{n-1} \sum_{i=1}^{n-1} (\mathbf{x}^{(i+1)} - \mathbf{x}^{(i)})^t \Sigma^{-1} (\mathbf{x}^{(i+1)} - \mathbf{x}^{(i)}),$$

which is proportional to the unweighted sum of the lag-1 autocorrelations over the principal components of the ellipse. The theoretical expectation of the MSJD at stationarity is known as the expected squared jump distance (ESJD).

Figure 1 shows traceplots for three different Markov chains. Estimates of the autocorrelation from lag-0 to lag-40 for each Markov chain appear alongside the corresponding traceplot. The simple window estimator for integrated ACT provides estimates of, respectively, 39.7, 5.5, and 35.3. The MSEJDs are, respectively, 0.027, 0.349, and 0.063, and are equal to the MSJDs since the stationary distribution has a variance of 1.

2.2.3 *Assessing accuracy.* An MCMC algorithm might efficiently explore an unimportant part of the parameter space and never find the main posterior mass. ACT's will be low, therefore, but the resulting posterior

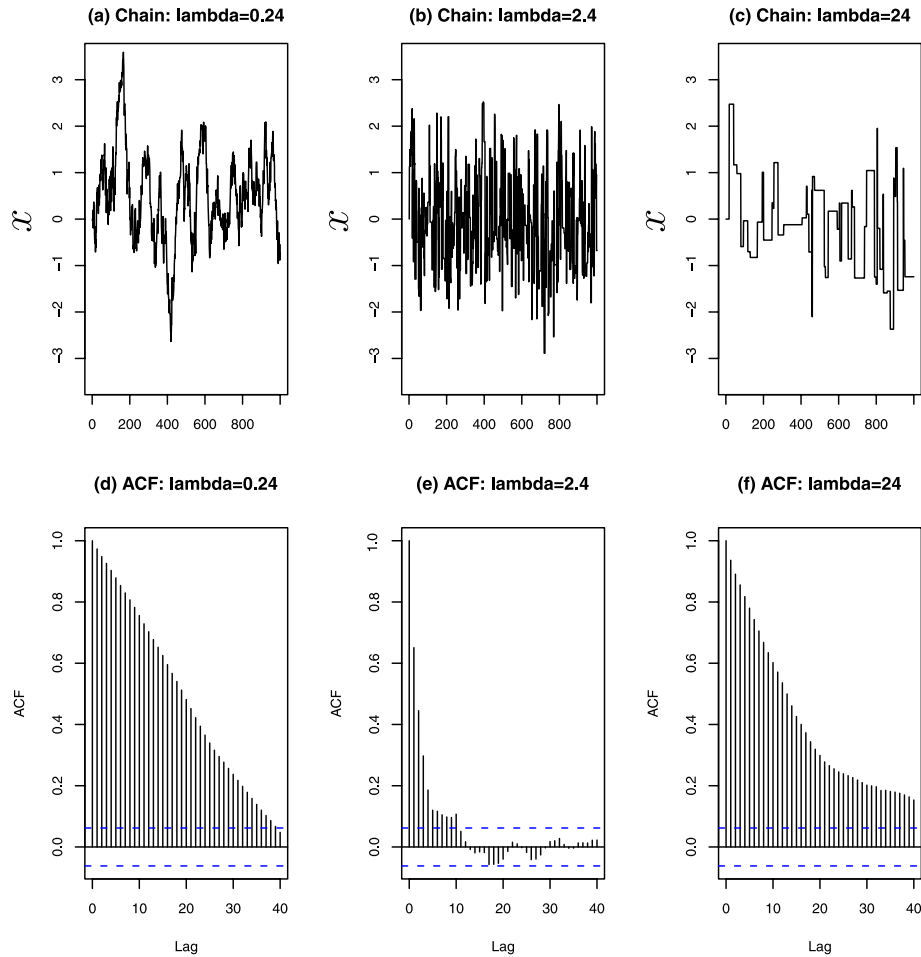


FIG. 1. Traceplots [(a), (b), and (c)] and corresponding autocorrelation plots [(d), (e), and (f)], for exploration of a standard Gaussian initialized from  $x = 0$  and using the random walk Metropolis algorithm with Gaussian proposal for 1000 iterations. Proposal scale parameters for the three scenarios are, respectively, (a) and (d) 0.24, (b) and (e) 2.4, and (c) and (f) 24.

estimate will be wildly inaccurate. In most practical examples it is not possible to determine the accuracy of the posterior estimate, though consistency between several independent runs or between different portions of the same run can be tested.

For the purposes of this article it was important to have a relatively accurate estimate of the posterior, not determined by a RWM algorithm. Fearnhead and Sherlock (2006) detailed a Gibbs sampler for the MMPP; this Gibbs sampler was run for 100,000 iterations on each of the datasets analyzed in this article. A “burn in” of 1000 iterations was allowed for, and a posterior estimate from the last 99,000 iterations was used as a reference for comparison with posterior estimates from RWM runs of 10,000 iterations (after burn in).

*2.2.4 Theoretical approaches for algorithm efficiency.* To date, theoretical results on the efficiency of RWM algorithms have been obtained through two

very different approaches. We wish to quote, explain, and apply theory from both and so we give a heuristic description of each and define associated notation. Both approaches link some measure of efficiency to the expected acceptance rate—the expected proportion of proposals accepted at stationarity.

The first approach was pioneered by Roberts, Gelman and Gilks (1997) for targets with independent identically distributed components and then generalized by Roberts and Rosenthal (2001) to targets of the form

$$\pi(\mathbf{x}) = \prod_1^d C_i f(C_i x_i).$$

The inverse scale parameters,  $C_i$ , are assumed to be drawn from some distribution with a given (finite) mean and variance. A single component of the  $d$ -dimensional chain (without loss of generality the first)

is then examined; at iteration  $i$  of the algorithm it is denoted  $X_{1,i}^{(d)}$ . A scaleless, speeded up, continuous-time process which mimics the first component of the chain is defined as

$$W_t^{(d)} := C_1 X_{1,[td]}^{(d)},$$

where  $[u]$  denotes the nearest integer less than or equal to  $u$ . Finally, proposed jumps are assumed to be Gaussian

$$\mathbf{Y}^{(d)} \sim N(\mathbf{0}, \lambda_d^2 \mathbf{I}).$$

Subject to conditions on the first two derivatives of  $f(\cdot)$ , Roberts and Rosenthal (2001) showed that if  $\mathbb{E}[C_i] = 1$  and  $\mathbb{E}[C_i^2] = b$ , and provided  $\lambda_d = \mu/d^{1/2}$  for some fixed  $\mu$  (the scale parameter but “rescaled” according to dimension), then as  $d \rightarrow \infty$ ,  $W_t^{(d)}$  approaches a Langevin diffusion process with speed

$$(9) \quad h(\mu) = \frac{C_1^2 \mu^2}{b} \bar{\alpha}_d$$

where  $\bar{\alpha}_d := 2\Phi\left(-\frac{1}{2}\mu J^{1/2}\right)$ .

Here  $\Phi(x)$  is the cumulative distribution function of a standard Gaussian,  $J := \mathbb{E}[(\log f)']^2$  is a measure of the roughness of the target, and  $\bar{\alpha}_d$  corresponds to the acceptance rate.

Bédard (2007) proved a similar result for a triangular sequence of inverse scale parameters  $c_{i,d}$ , which are assumed to be known. A necessary and sufficient condition equivalent to (11) below is attached to this result. In effect this requires the scale over which the smallest component varies to be “not too much smaller” than the scales of the other components.

The second technique (e.g., Sherlock and Roberts, 2009) uses expected squared jump distance (ESJD) as a measure of efficiency. Exact analytical forms for ESJD (denoted  $S_d^2$ ) and expected acceptance rate are derived for any unimodal elliptically symmetric target and any proposal density. Many standard sequences of  $d$ -dimensional targets ( $d = 1, 2, \dots$ ), such as the Gaussian, satisfy the condition that as  $d \rightarrow \infty$  the probability mass becomes concentrated in a spherical shell which itself becomes infinitesimally thin relative to its radius. Thus the random walk on a rescaling of the target is, in the limit, effectively confined to the surface of this shell. Sherlock and Roberts (2009) considered a sequence of targets which satisfies such a “shell” condition, and a sequence of proposals which satisfies a slightly stronger condition. Specifically it is re-

quired that there exist sequences of positive real numbers,  $\{k_x^{(d)}\}$  and  $\{k_y^{(d)}\}$ , such that

$$\frac{\|\mathbf{X}^{(d)}\|}{k_x^{(d)}} \xrightarrow{p} 1 \quad \text{and} \quad \frac{\|\mathbf{Y}^{(d)}\|}{\lambda_d k_y^{(d)}} \xrightarrow{\text{m.s.}} 1.$$

For such combinations of target and proposal, as  $d \rightarrow \infty$

$$(10) \quad \frac{d}{k_x^{(d)2}} S_d^2(\mu) \rightarrow \mu^2 \bar{\alpha}_d$$

with  $\bar{\alpha}_d(\mu) := 2\Phi\left(-\frac{1}{2}\mu\right)$ .

Here  $\bar{\alpha}_d$  is the limiting expected acceptance rate, and  $\mu := d^{1/2} \lambda_d k_y^{(d)} / k_x^{(d)}$ . For target and proposal distributions with independent components, such as are used in the diffusion results,  $k_x^{(d)} = k_y^{(d)} = d^{1/2}$ , and hence (consistently)  $\mu = d^{1/2} \lambda_d$ .

It is also required that the elliptical target not be too eccentric. Specifically, for a sequence of target densities  $\pi_d(\mathbf{x}) := f_d(\sum_{i=1}^d c_{i,d}^2 x_i^2)$  (for some appropriate sequence of functions  $\{f_d\}$ )

$$(11) \quad \frac{\max_i c_{i,d}^2}{\sum_{i=1}^d c_{i,d}^2} \rightarrow 0 \quad \text{as } d \rightarrow \infty.$$

Theoretical results from the two techniques are remarkably similar and as will be seen, lead to identical strategies for optimizing algorithm efficiency. It is worth noting, however, that results from the first approach apply only to targets with independent components and results from the second only to targets which are unimodal and elliptically symmetric. That they lead to identical strategies indicates a certain potential robustness of these strategies to the form of the target. This potential, as we shall see, is borne out in practice.

### 2.3 The Markov Modulated Poisson Process

Let  $X_t$  be a continuous-time Markov chain on discrete state space  $\{1, \dots, d\}$  and let  $\boldsymbol{\psi} := [\psi_1, \dots, \psi_d]$  be a  $d$ -dimensional vector of (nonnegative) intensities. The linked but stochastically independent Poisson process  $Y_t$  whose intensity is  $\psi_{X_t}$  is a Markov modulated Poisson process—it is a Poisson process whose intensity is modulated by a continuous-time Markov chain.

The idea is best illustrated through two examples, which also serve to introduce the notation and datasets that will be used throughout this article. Consider a two-dimensional Markov chain  $X_t$  with generator  $\mathbf{Q}$  with  $q_{12} = q_{21} = 1$ .

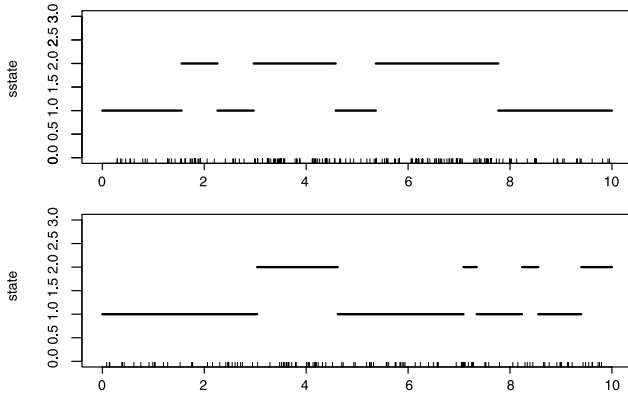


FIG. 2. Two 2-state continuous-time Markov chains simulated for 10 seconds from generator  $\mathbf{Q}$  with  $q_{12} = q_{21} = 1$ ; the rug plots show events from an MMPP simulated from these chains, with intensity vectors  $\boldsymbol{\psi} = [10, 30]$  (upper graph) and  $\boldsymbol{\psi} = [10, 17]$  (lower graph).

Figure 2 shows realizations from two such chains over a period of 10 seconds. Now consider a Poisson process  $Y_t$  which has intensity 10 when  $X_t$  is in state 1 and intensity 30 when  $X_t$  is in state 2. This is an MMPP with event intensity vector  $\boldsymbol{\psi} = [10, 30]$ . A realization (obtained via the realization of  $X_t$ ) is shown as a rug plot underneath the chain in the upper graph. The lower graph shows a realization from an MMPP with event intensities  $[10, 17]$ .

It can be shown (e.g., Fearnhead and Sherlock, 2006) that the likelihood for data from an MMPP which starts from a distribution  $\boldsymbol{\nu}$  over its states is

$$L(\mathbf{Q}, \boldsymbol{\Psi}, \mathbf{t}) = \boldsymbol{\nu}' e^{(\mathbf{Q}-\boldsymbol{\Psi})t_1} \boldsymbol{\Psi} \dots e^{(\mathbf{Q}-\boldsymbol{\Psi})t_n} \boldsymbol{\Psi} e^{(\mathbf{Q}-\boldsymbol{\Psi})t_{n+1}} \mathbf{1}. \tag{12}$$

Here  $\boldsymbol{\Psi} := \text{diag}(\boldsymbol{\psi})$ ,  $\mathbf{1}$  is a vector of 1's,  $n$  is the number of observed events,  $t_1$  is the time from the start of the observation window until the first event,  $t_{n+1}$  is the time from the last event until the end of the observation window, and  $t_i$  ( $2 \leq i \leq n$ ) is the time between the  $(i-1)$ th and  $i$ th events. In the absence of further information, the initial distribution  $\boldsymbol{\nu}$  is often taken to be the stationary distribution of the underlying Markov chain.

The likelihood of an MMPP is invariant to a re-labeling of the states. Hence if the prior is similarly invariant, then so too is the posterior: if the posterior for a two-dimensional MMPP has a mode at  $(\psi_1, \psi_2, q_{12}, q_{21})$ , then it has an identical mode at  $(\psi_2, \psi_1, q_{21}, q_{12})$ . In this article our overriding interest is in the efficiency of the MCMC algorithms rather than the exact meaning of the parameters and so we choose the simplest solution to this identifiability problem: the state with the lower Poisson intensity  $\psi$  is always referred to as state 1.

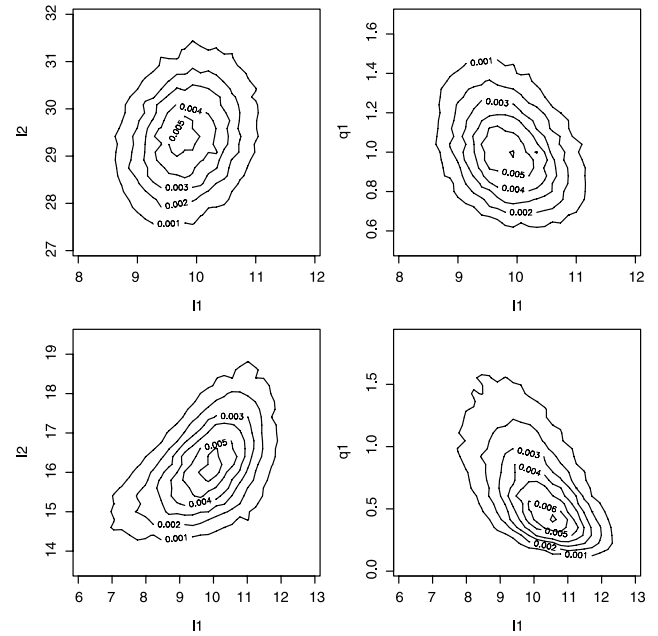


FIG. 3. Estimated marginal posteriors for  $\psi_1$  and  $\psi_2$  and for  $\psi_1$  and  $q_{12}$  from long runs of the Gibbs sampler for datasets D1 (top) and D2 (bottom).

2.3.1 *MMPP data in this article.* The two datasets of event times used in this article arose from two independent MMPP's simulated over an observation window of 100 seconds. Both underlying Markov chains have  $q_{12} = q_{21} = 1$ ; dataset D1 has event intensity vector  $\boldsymbol{\psi} = [10, 30]$  whereas dataset D2 has  $\boldsymbol{\psi} = [10, 17]$ , so that the overall intensity of events in D2 is lower than in D1. As mentioned in Section 2.2.3, a posterior sample from a long run of the Gibbs sampler of Fearnhead and Sherlock (2006) was used to approximate the true posterior. Figure 3 shows estimates of the marginal posterior distribution for  $(\psi_1, \psi_2)$  and for  $(\psi_1, q_{12})$  for D1 (top) and D2 (bottom).

Because the difference in intensity between the states is so much larger in D1 than in D2 it is easier with D1 than D2 to distinguish the state of the underlying Markov chain, and thus the values of the Markov and Poisson parameters. Further, in the limit of the underlying chain being known precisely, for example as  $\psi_2 \rightarrow \infty$  with  $\psi_1$  finite, and provided the priors are independent, the posteriors for the Poisson intensity parameters  $\psi_1$  and  $\psi_2$  are completely independent of each other and of the Markov parameters  $q_{12}$  and  $q_{21}$ . Dependence between the Markov parameters is also small, being  $O(1/T)$  (e.g., Fearnhead and Sherlock, 2006).

In Section 4, differences between D1 and D2 will be related directly to observed differences in efficiency of the various RWM algorithms between the two datasets.

### 3. IMPLEMENTATIONS OF THE RWM: THEORY AND PRACTICE

This section describes several theoretical results for the RWM or for MCMC in general. Intuitive explanation of the principle behind each result is emphasized and the manner in which it informs the RWM implementation is made clear. Each algorithm was run three times on each of the two datasets.

#### 3.1 Optimal Scaling of the RWM

*Intuition:* Consider the behavior of the RWM as a function of the overall scale parameter of the proposed jump,  $\lambda$ , in (1). If most proposed jumps are small compared with some measure of the scale of variability of the target distribution, then, although these jumps will often be accepted, the chain will move slowly and exploration of the target distribution will be relatively inefficient. If the jumps proposed are relatively large compared with the target distribution's scale, then many will not be accepted, the chain will rarely move, and will again explore the target distribution inefficiently. This suggests that given a particular target and form for the jump proposal distribution, there may exist a finite scale parameter for the proposal with which the algorithm will explore the target as efficiently as possible. These ideas are clearly demonstrated in Figure 1 which shows traceplots for a one-dimensional Gaussian target explored using a Gaussian proposal with scale parameter an order of magnitude smaller (a) and larger (c) than is optimal, and (b) with a close to optimal scale parameter.

*Theory:* Equation (9) gives algorithm efficiency for a target with independent and identical (up to a scaling) components as a function of the "rescaled" scale parameter  $\mu = d^{1/2}\lambda_d$  of a Gaussian proposal. Equation (10) gives algorithm efficiency for a unimodal elliptically symmetric target explored by a spherically symmetric proposal with  $\mu = d^{1/2}\lambda_d k_y^{(d)}/k_x^{(d)}$ . Efficiencies are therefore optimal at  $\mu \approx 2.38/J^{1/2}$  and  $\mu \approx 2.38$ , respectively. These correspond to actual scale parameters of respectively

$$\lambda_d = \frac{2.38}{J^{1/2}d^{1/2}} \quad \text{and} \quad \lambda_d = \frac{2.38k_x^{(d)}}{d^{1/2}k_y^{(d)}}.$$

The equivalence between these two expressions for Gaussian data explored with a Gaussian target is clear from Section 2.2.4. However, the equations offer little direct help in choosing a scale parameter for a target which is neither elliptical nor possesses components which are i.i.d. up to a scale parameter. Substitution of

each expression into the corresponding acceptance rate equation, however, leads to the same optimal acceptance rate,  $\hat{\alpha} \approx 0.234$ . This justifies the relatively well-known adage that *for random walk algorithms with a large number of parameters, the scale parameter of the proposal should be chosen so that the acceptance rate is approximately 0.234*. On a graph of asymptotic efficiency against acceptance rate (e.g., Roberts and Rosenthal, 2001), the curvature near the mode is slight, especially to its right, so that an acceptance rate of anywhere between 0.2 and 0.3 should lead to an algorithm of close to optimal efficiency.

In practice updates are performed on a finite number of parameters; for example, a two-dimensional MMPP has four parameters ( $\psi_1, \psi_2, q_{12}, q_{21}$ ). A block update involves all of these, while each update of a simple Metropolis-within-Gibbs step involves just one parameter. In finite dimensions the optimal acceptance rate can in fact take any value between 0 and 1. Sherlock and Roberts (2009) provided analytical formulas for calculating the ESJD and the expected acceptance rate for any proposal and any elliptically symmetric unimodal target. In one dimension, for example, the optimal acceptance rate for a Gaussian target explored by a Gaussian proposal is 0.44, while the optimum for a Laplace target ( $\pi(x) \propto e^{-|x|}$ ) explored with a Laplace proposal is exactly  $\hat{\alpha} = 1/3$ . Sherlock (2006) considered several simple examples of spherically symmetric proposal and target across a range of dimensions and found that in all cases curvature at the optimal acceptance rate is small, so that a range of acceptance rates is nearly optimal. Further, the optimal acceptance rate is itself between 0.2 and 0.3 for  $d \geq 6$  in all the cases considered.

Sherlock and Roberts (2009) also weakened the "shell" condition of Section 2.2.4 and considered sequences of spherically symmetric targets for which the (rescaled) radius converges to some random variable  $R$  rather than a point mass at 1. It is shown that, provided the sequence of proposals still satisfies the shell condition, the limiting optimal acceptance rate is strictly less than 0.234. Acceptance rate tuning should thus be seen as only a guide, though a guide which has been found to be robust in practice.

ALGORITHM 1 (Blk). The first algorithm (Blk) used to explore datasets D1 and D2 is a four-dimensional block updating RWM with proposal  $\mathbf{Y} \sim N(0, \lambda^2 \mathbf{I})$  and  $\lambda$  tuned so that the acceptance rate is approximately 0.3.



### 3.2 Optimal Scaling of the RWM-Within-Gibbs

*Intuition:* Consider first a target either spherically symmetric, or with i.i.d. components, and let the overall scale of variability of the target be  $\eta$ . For full block proposals the optimal scale parameter should be  $O(\eta/d^{1/2})$  so that the square of the magnitude of the total proposal is  $O(\eta^2)$ . If a Metropolis-within-Gibbs update is to be used with  $k$  sub-blocks and  $d_* = d/k$  of the components updated at each stage, then the optimal scale parameter should be larger,  $O(\eta/d_*^{1/2})$ . However, only one of the  $k$  stages of the RWM-within-Gibbs algorithm updates any given component whereas with  $k$  repeats of a block RWM that component is updated  $k$  times. Considering the squared jump distances it is easy to see that, given the additivity of squared jump distances, the larger size of the RWM-within-Gibbs updates is exactly canceled by their lower frequency, and so (in the limit) there is no difference in efficiency when compared with a block update. The same intuition applies when comparing a random scan Metropolis-within-Gibbs scheme with a single block update.

Now consider a target for which different components vary on different scales. If sub-blocks are chosen so as to group together components with similar scales, then a Metropolis-within-Gibbs scheme can apply suitable scale parameters to each block whereas a single block update must choose one scale parameter that is adequate for all components. In this scenario, Metropolis-within-Gibbs updates should therefore be more efficient.

*Theory:* Neal and Roberts (2006) considered a random scan RWM-within-Gibbs algorithm on a target distribution with i.i.d. components and using i.i.d. Gaussian proposals all having the same scale parameter  $\lambda_d = \mu/d^{1/2}$ . At each iteration a fraction,  $\gamma_d$ , of the  $d$  components are chosen uniformly at random and updated as a block. It is shown [again subject to differentiability conditions on  $f(\cdot)$ ] that the process  $W_t^{(d)} := X_{1,[td]}^{(d)}$  approaches a Langevin diffusion with speed

$$h_\gamma(\mu) = 2\gamma\mu^2\Phi(-\frac{1}{2}\mu(\gamma J)^{1/2}),$$

where  $\gamma := \lim_{d \rightarrow \infty} \gamma_d$ . The optimal scaling is therefore larger than for a standard block update (by a factor of  $\gamma^{-1/2}$ ) but the optimal speed and the optimal acceptance rate (0.234) are identical to those found by Roberts, Gelman and Gilks (1997).

Sherlock (2006) considered sequential Metropolis-within-Gibbs updates on a unimodal elliptically symmetric target, using spherical proposal distributions

but allowing *different* scale parameters for the proposals in each sub-block. The  $k$  sub-blocks are assumed to correspond to disjoint subsets of the principal axes of the ellipse and updates for each are assumed to be optimally tuned. Efficiency is considered in terms of ESEJD and is again found to be optimal (as  $d \rightarrow \infty$ ) when the acceptance rate for each sub-block is 0.234. For equal sized sub-blocks, the relative efficiency of the Metropolis-within-Gibbs scheme compared to  $k$  optimally scaled single block updates is shown to be

$$(13) \quad r = \frac{(1/k) \sum \overline{c^2_i}}{((1/k) \sum 1/\overline{c^2_i})^{-1}},$$

where  $\overline{c^2_i}$  is the mean of the squares of the inverse scale parameters for the  $i$ th block. Since  $r$  is the ratio of an arithmetic mean to a harmonic mean, it is greater than or equal to 1 and thus the Metropolis-within-Gibbs step is always at least as efficient as the block Metropolis. However, the more similar the blocks, the less the potential gain in efficiency.

In practice, parameter blocks do not generally correspond to disjoint subsets of the principal axes of the posterior or, in terms of single parameter updates, the parameters are not generally orthogonal. Equation (13) therefore corresponds to a limiting maximum efficiency gain, obtainable only when the parameter sub-blocks are orthogonal.

ALGORITHM 2 (MwG). Our second algorithm (MwG) is a sequential Metropolis-within-Gibbs algorithm with proposed jumps  $Y_i \sim N(0, \lambda_i^2)$ . Each scale parameter is tuned separately to give an acceptance rate of between 0.4 and 0.45 (approximately the optimum for a one-dimensional Gaussian target and proposal).

### 3.3 Tailoring the Shape of a Block Proposal

*Intuition:* First consider a two-dimensional target with roughly elliptical contours and with the scale of variation along one of the principal axes much larger than the scale of variation along the other (e.g., the two right-hand panels of Figure 3). The size of updates from a proposal of the type used in Algorithm 1 is constrained by the smaller of the two scales of variation. Thus, even when Algorithm 1 is optimally tuned, the efficiency of exploration along the larger axis depends on the ratio of the two scales and so can be arbitrarily low in targets where this ratio is large. Now consider a general target with roughly elliptical contours and covariance matrix  $\Sigma$ . It seems intuitively sensible that

a “tailored” block proposal distribution with the same shape and orientation as the target will tend to produce larger jumps along the target’s major axes and smaller jumps along its minor axes and should therefore allow for more efficient exploration of the target.

*Theory:* Sherlock (2006) considered exploration of a unimodal elliptically symmetric target with either a spherically symmetric proposal or a tailored elliptically symmetric proposal in the limit as  $d \rightarrow \infty$ . Subject to condition (11) (and a “shell”-like condition similar to that mentioned in Section 2.2.4), it is shown that with each proposal shape it is in fact possible to achieve the same optimal expected squared jump distance. However, if a spherically symmetric proposal is used on an elliptical target, some components are explored better than others and in some sense the overall efficiency is reduced. This becomes clear on considering the ratio,  $r$ , of the expected squared Euclidean jump distance for an optimal spherically symmetric proposal to that of an optimal tailored proposal. Sherlock (2006) showed that for a sequence of targets, where the target with dimension  $d$  has elliptical axes with inverse scale parameters  $c_{d,1}, \dots, c_{d,d}$ , the limiting ratio is

$$r = \frac{\lim_{d \rightarrow \infty} ((1/d) \sum_{i=1}^d c_{d,i}^{-2})^{-1}}{\lim_{d \rightarrow \infty} (1/d) \sum_{i=1}^d c_{d,i}^2}.$$

The numerator is the limiting harmonic mean of the squared inverse scale parameters, which is less than or equal to their arithmetic mean (the denominator), with equality if and only if (for a given  $d$ ) all the  $c_{d,i}$  are equal. Roberts and Rosenthal (2001) examined similar relative efficiencies but for targets and proposals with independent components with inverse scale parameters  $C$  sampled from some distribution. In this case the derived measure of relative efficiency is the relative speeds of the diffusion limits for the first component of the target

$$r^* = \frac{\mathbb{E}[C]^2}{\mathbb{E}[C^2]}.$$

This is again less than or equal to 1, with equality when all the scale parameters are equal. Hence efficiency is indeed directly related to the relative compatibility between target and proposal shapes.

Furthermore, Bédard (2008) showed that if a proposal has i.i.d. components yet the target (assumed to have independent components) is wildly asymmetric, as measured by (11), then the limiting optimal acceptance rate can be anywhere between 0 and 1. However, even at this optimum, some components will be explored infinitely more slowly than others.

In practice the shape  $\Sigma$  of the posterior is not known and must be estimated, for example by numerically finding the posterior mode and the Hessian matrix  $\mathbf{H}$  at the mode, and setting  $\Sigma = \mathbf{H}^{-1}$ . We employ a simple alternative which uses an earlier MCMC run.

**ALGORITHM 3 (BlkShp).** Our third algorithm first uses an optimally scaled block RWM algorithm (Algorithm 1), which is run for long enough to obtain a “reasonable” estimate of the covariance from the posterior sample. A fresh run is then started and tuned to give an acceptance rate of about 0.3 but using proposals

$$\mathbf{Y} \sim N(\mathbf{0}, \lambda^2 \hat{\Sigma}).$$

For each dataset, so that our implementation would reflect likely statistical practice, each of the three replicates of this algorithm estimated the  $\Sigma$  matrix from iterations 1000–2000 of the corresponding replicate of Algorithm 1 (i.e., using 1000 iterations after “burn in”). In all, therefore, six different variance matrices were used.

### 3.4 Improving Tail Exploration

*Intuition:* A posterior with relatively heavy polynomial tails such as the one-dimensional Cauchy distribution has considerable mass some distance from the origin. Proposal scalings which efficiently explore the body of the posterior are thus too small to explore much of the tail mass in a “reasonable” number of iterations. Further, polynomial tails become flatter with distance from the origin so that for unit vector  $\mathbf{u}$ ,  $\pi(\mathbf{x} + \lambda \mathbf{u})/\pi(\mathbf{x}) \rightarrow 1$  as  $\|\mathbf{x}\|_2 \rightarrow \infty$ . Hence the acceptance rate for a random walk algorithm approaches 1 in the tails, whatever the direction of the proposed jump. The algorithm therefore loses almost all sense of the direction to the posterior mass.

*Theory:* Roberts (2003) brought together literature relating the tails of the  $d$ -dimensional posterior and proposal to the ergodicity of the Markov chain and hence its convergence properties. Three important cases are noted:

- (1) If  $\exists s > 0$  such that  $\pi(\mathbf{x}) \propto e^{-s\|\mathbf{x}\|_2}$ , at least outside some compact set, then the random walk algorithm is geometrically ergodic.
- (2) If  $\exists r > 0$  such that the tails of the proposal are bounded by some multiple of  $\|x\|_2^{-(r+d)}$  and if  $\pi(\mathbf{x}) \propto \|\mathbf{x}\|_2^{-(r+d)}$ , at least outside some compact set, then the algorithm is polynomially ergodic with rate  $r/2$ .

- (3) If  $\exists r > 0$  and  $\eta \in (0, 2)$  such that  $\pi(\mathbf{x}) \propto \|\mathbf{x}\|_2^{-(r+d)}$ , at least for large enough  $\mathbf{x}$ , and the proposal has tails  $q(\mathbf{x}) \propto \|\mathbf{x}\|_2^{-(d+\eta)}$ , then the algorithm is polynomially ergodic with rate  $r/\eta$ .

Thus posterior distributions with exponential or lighter tails lead to a geometrically ergodic Markov chain, whereas polynomially tailed posteriors can lead to polynomially ergodic chains, and even this is only guaranteed if the tails of the proposal are at least as heavy as the tails of the posterior. However, by using a proposal with tails so heavy that it has infinite variance, the polynomial convergence rate can be made as large as is desired.

**ALGORITHM 4 (BlkShpCau).** Our fourth algorithm is identical to BlkShp but samples the proposed jump from the heavy-tailed multivariate Cauchy. Proposals are generated by simulating  $\mathbf{V} \sim N(\mathbf{0}, \hat{\Sigma})$  and  $Z \sim N(0, 1)$  and setting  $\mathbf{Y}^* = \mathbf{V}/Z$ . No acceptance rate criteria exist for proposals with infinite variance and so the optimal scaling parameter for this algorithm was found (for each dataset and  $\hat{\Sigma}$ ) by repeating several small runs with different scale parameters and noting which produced the best ACT's for each dataset.

**ALGORITHM 5 (BlkShpMul).** The fifth algorithm relies on the fact that taking logarithms of parameters shifts mass from the tails to the center of the distribution. It uses a random walk on the posterior of  $\tilde{\theta} := (\log \psi_1, \log \psi_2, \log q_{12}, \log q_{21})$ . Shape matrices  $\tilde{\Sigma}$  were estimated as for Algorithm 3, but using the logarithms of the posterior output from Algorithm 1. In the original parameter space this algorithm is equivalent to a proposal with components  $X_i^* = X_i e^{Y_i^*}$  and so has been called the *multiplicative random walk* (see, e.g., Dellaportas and Roberts, 2003). In the original parameter space the acceptance probability is

$$\alpha(\mathbf{x}, \mathbf{x}^*) = \min\left(1, \frac{\prod_1^d x_i^* \pi(\mathbf{x}^*)}{\prod_1^d x_i \pi(\mathbf{x})}\right).$$

Since the algorithm is simply an additive random walk on the log parameter space, the usual acceptance rate optimality criteria apply.

A logarithmic transformation is clearly only appropriate for positive parameters and can in fact lead to a heavy left-hand tail if a parameter (in the original space) has too much mass close to zero. The transformation  $\tilde{\theta}_i = \text{sign}(\theta_i) \log(1 + |\theta_i|)$  circumvents both of these problems.

### 3.5 Additional Strategies

Scaling and shaping of the proposal, the choice of proposal distribution (here Gaussian or Cauchy), and an informed choice between RWM and Metropolis-within-Gibbs updates can all lead to a more efficient algorithm. Building on these possibilities, we now consider two further mechanisms for improving efficiency: adaptive MCMC, and utilizing problem-specific knowledge.

#### 3.5.1 Adaptive MCMC.

*Intuition:* Algorithm 3 used the output from a previous MCMC run to estimate the shape Matrix  $\Sigma$ . An overall scaling parameter was then varied to give an acceptance rate of around 0.3. With adaptive MCMC a single chain is run, and this chain gradually alters its own proposal distribution (e.g., changing  $\Sigma$ ), by learning about the posterior *from its own output*. This simple idea has a major potential pitfall, however.

If the algorithm is started away from the main posterior mass, for example in a tail or a minor mode, then it initially learns about that region. It therefore alters the proposal so that it efficiently explores this region of minor importance. Worse, in so altering the proposal the algorithm may become even less efficient at finding the main posterior mass, remain in an unimportant region for longer, and become even more influenced by that unimportant region. Since the transition kernel is continually changing, potentially with this positive feedback mechanism, it is no longer guaranteed that the overall stationary distribution of the chain is  $\pi(\cdot)$ .

A simple solution is so-called *finite adaptation* wherein the algorithm is only allowed to evolve for the first  $n_0$  iterations, after which time the transition kernel is fixed. Such a scheme is equivalent to running a shorter ‘‘tuning’’ chain and then a longer subsequent chain (e.g., Algorithm 3). If the tuning portion of the chain has only explored a minor mode or a tail, this still leads to an inefficient algorithm. We would prefer to allow the chain to eventually correct for any errors made at early iterations and yet still lead to the intended stationary distribution. It seems sensible that this might be achieved provided changes to the kernel become smaller and smaller as the algorithm proceeds and provided the above-mentioned positive feedback mechanism can never pervert the entire algorithm.

*Theory:* At the  $n$ th iteration let  $\Gamma_n$  represent the choice of transition kernel; for the RWM it might represent the current shape matrix  $\Sigma$  and the overall scaling  $\lambda$ . Denote the corresponding transition kernel  $P_{\Gamma_n}(\mathbf{x}, \cdot)$ . Roberts and Rosenthal (2007) derived two

conditions which together guarantee convergence to the stationary distribution. A key concept is that of *diminishing adaptation*, wherein changes to the kernel must become vanishingly small as  $n \rightarrow \infty$ ,

$$\sup_{\mathbf{x}} \|P_{\Gamma_{n+1}}(\mathbf{x}, \cdot) - P_{\Gamma_n}(\mathbf{x}, \cdot)\|_1 \xrightarrow{p} 0 \quad \text{as } n \rightarrow \infty.$$

A second *containment* condition considers the  $\varepsilon$ -convergence time under repeated application of a fixed kernel,  $\gamma$ , and starting point  $\mathbf{x}$ ,

$$M_\varepsilon(\mathbf{x}, \gamma) := \inf_n \{n \geq 1 : \|P_\gamma^n(\mathbf{x}, \cdot) - \pi(\cdot)\|_1 \leq \varepsilon\},$$

and requires that for all  $\delta > 0$  there is an  $N$  such that for all  $n$

$$\mathbb{P}(M_\varepsilon(\mathbf{X}_n, \Gamma_n) \leq N | \mathbf{X}_0 = \mathbf{x}_0, \Gamma_0 = \gamma_0) \geq 1 - \delta.$$

The containment condition is difficult to check in practice; some criteria are provided in the work of Bai, Roberts and Rosenthal (2009).

Adaptive MCMC is a highly active research area and so we confine ourselves to an adaptive version of Algorithm 5. Roberts and Rosenthal (2010) described an adaptive RWM algorithm for which the proposal at the  $n$ th iteration is sampled from a mixture of an adaptive  $N(\mathbf{0}, \frac{1}{d} 2.38^2 \tilde{\Sigma}_n)$  and a nonadaptive Gaussian distribution; here  $\tilde{\Sigma}_n$  is the variance matrix calculated from the previous  $n - 1$  iterations of the scheme. Changes to the variance matrix are  $O(1/n)$  at the  $n$ th iteration and so the algorithm satisfies the diminishing adaptation condition.

Choice of the overall scaling factor  $2.38^2/d$  follows directly from the optimal scaling limit results reviewed in Section 3.1, with  $J = 1$  or  $k_x^{(d)} = k_y^{(d)}$ . In general, therefore, a different scaling might be appropriate, and so our scheme extends that of Roberts and Rosenthal (2010) by allowing the overall scaling factor to adapt.

**ALGORITHM 6** (BlkAdpMul). Our adaptive MCMC algorithm is a block multiplicative random walk which samples jump proposals on the log-posterior from the mixture

$$\mathbf{Y} \sim \begin{cases} N(\mathbf{0}, m_n^2 \tilde{\Sigma}_n) & \text{w.p. } 1 - \delta, \\ N(\mathbf{0}, \frac{1}{d} \lambda_0^2 \mathbf{I}) & \text{w.p. } \delta. \end{cases}$$

Here  $\delta = 0.05$ ,  $d = 4$ , and  $\tilde{\Sigma}_n$  is the variance matrix of the logarithms of the posterior sample to date. A few minutes were spent tuning the block multiplicative random walk with proposal variance  $\frac{1}{4} \lambda_0^2 \mathbf{I}$  to give at least a reasonable value for  $\lambda_0$  (acceptance rate  $\approx 0.3$ ), although this is not strictly necessary.

To ensure a sensible nonsingular  $\tilde{\Sigma}_n$ , proposals from the adaptive part of the mixture were only allowed once there had been at least 10 proposed jumps accepted. The overall scaling factor for the adaptive part of the kernel,  $m_n$ , was initialized to  $m_0 = 2.38/d^{1/2}$  and an adaptation quantity  $\Delta = m_0/100$  was defined. If iteration  $i$  was from the nonadaptive part of the kernel, then  $m_{i+1} \leftarrow m_i$ ; otherwise:

- If the proposal was rejected, then  $m_{i+1} \leftarrow m_i - \Delta/i^{1/2}$ .
- If the proposal was accepted, then  $m_{i+1} \leftarrow m_i + 2.3\Delta/i^{1/2}$ .

This leads to an equilibrium acceptance rate of  $1/3.3 \approx 30\%$ , the target acceptance rate for the other block updating algorithms which use Gaussian proposals (Algorithms 1, 3, and 5). Changes to  $m$  are scaled by  $i^{1/2}$  since they must be large enough to adapt to changes in the covariance matrix yet small enough that an equilibrium value is established relatively quickly. As with the variance matrix, such a value would then only change noticeably if there were consistent evidence that it should.

### 3.5.2 Utilizing problem-specific knowledge.

*Intuition:* Algorithms are always applied to specific datasets with specific forms for the likelihood and prior. Combining techniques such as optimal scaling and shape adjustment with problem-specific knowledge can often markedly improve efficiency. In the case of the MMPP we define a reparameterization based on the intuition that for an MMPP with  $\psi_1 \approx \psi_2$  (as in D2) the data contain a great deal of information about the average intensity but relatively little information about the difference between the intensities.

*Theory:* For a two-dimensional MMPP define an overall transition intensity, stationary distribution, mean intensity at stationarity, and a measure of the difference between the two event intensities as follows:

$$(14) \quad \begin{aligned} q &:= q_{12} + q_{21}, & \mathbf{v} &:= \frac{1}{q} [q_{21}, q_{12}], \\ \bar{\psi} &:= \mathbf{v}^t \boldsymbol{\psi} & \text{and } \delta &:= \frac{(\psi_2 - \psi_1)}{\bar{\psi}}. \end{aligned}$$

Let  $t_{\text{obs}}$  be the total observation time and  $\mathbf{t}$  the vector of observed event times. If the Poisson event intensities are similar,  $\delta$  is small, and Taylor expansion of the log-likelihood in  $\delta$  (see Sherlock, 2006) gives

$$(15) \quad \begin{aligned} l(\bar{\psi}, q, \delta, v_1) & \\ &= n \log \bar{\psi} - \bar{\psi} t_{\text{obs}} + 2\delta^2 v_1 v_2 f(\bar{\psi} \mathbf{t}, q \mathbf{t}) \\ &\quad + \delta^3 v_1 v_2 (v_2 - v_1) g(\bar{\psi} \mathbf{t}, q \mathbf{t}) + O(\delta^4) \end{aligned}$$

for some  $f(\cdot, \cdot)$  and  $g(\cdot, \cdot)$ . Consider a reparameterization from  $(\psi_1, \psi_2, q_{12}, q_{21})$  to  $(\bar{\psi}, q, \alpha, \beta)$  with

$$(16) \quad \alpha := 2\delta(\nu_1\nu_2)^{1/2} \quad \text{and} \quad \beta := \delta(\nu_2 - \nu_1).$$

Parameters  $\bar{\psi}$ ;  $q$  and  $\alpha$ ; and  $\beta$  (in this order) capture decreasing amounts of variation in the log-likelihood and so, conversely, it might be anticipated that there be corresponding decreasing amounts of information about these parameters contained in the likelihood. Hence very different scalings might be required for each.

**ALGORITHM 7 (MwGRep).** A Metropolis-within-Gibbs update scheme was applied to the reparameterization  $(\bar{\psi}, q, \alpha, \beta)$ . A multiplicative random walk was used for each of the first three parameters (since they are positive) and an additive update was used for  $\beta$ . Scalings for each of the four parameters were chosen to give acceptance rates of between 0.4 and 0.45.

**ALGORITHM 8 (MwGRepCau).** Our final algorithm is identical to MwGRep except that additive updates for  $\beta$  are proposed from a *Cauchy* distribution. The Cauchy scaling was optimized to give the best ACT over the first 1000 iterations.

#### 4. RESULTS

The eight algorithms described in Section 3 are summarized in Table 1. The table includes two further algorithms, an independence sampler (Algorithm 9: IndShp), and the Gibbs sampler of Fearnhead and Sherlock (2006) (Algorithm 10: Gibbs); these were included to benchmark the efficiency of RWM algorithms against some sensible alternatives. The independence sampler used a multivariate  $t$  distribution with

five degrees of freedom and the same set of covariance matrices as Algorithm 3.

Each RWM variation was tested against datasets D1 and D2 as described in Section 2.3.1. For each dataset, each algorithm was started from the known “true” parameter values and was run three times with three different random seeds (referred to as Replicates 1–3). All algorithms were run for 11,000 iterations; a burn in of 1000 iterations was sufficient in all cases.

Priors were independent and exponential with means the known “true” parameter values. The likelihood of an MMPP with maximum and minimum Poisson intensities  $\psi_{\max}$  and  $\psi_{\min}$  and with  $n$  events observed over a time window of length  $t_{\text{obs}}$  is bounded above by  $\psi_{\max}^n e^{-\psi_{\min} t_{\text{obs}}}$ . In this article only MMPP parameters and their logarithms are considered for estimation. Since exponential priors are employed the parameters and their logarithms therefore have finite variance, and geometric ergodicity is guaranteed.

The accuracy of posterior simulations is assessed via QQ plot comparison with the output from a very long run of a Gibbs sampler (see Section 2.2.3). QQ plots for almost all replicates were almost entirely within their 95% confidence bounds. Figure 4 shows such plots for Algorithms 1–3 and 9 (the independence sampler) on dataset D2 (Replicate 1). In general these combinations produced the least accurate performance, and only with the independence sampler is there reason to doubt that the posterior sample is a reasonable representation of the true posterior. The relatively poor performance on D2 of Algorithms 1–3 and especially Algorithm 9 is repeated for the other two replicates. The third replicate of Algorithm 4 on D2 also showed an imperfect fit in the tails.

The integrated ACT was estimated for each parameter and each replicate using the final 10,000 iter-

TABLE 1  
Summary of the algorithms used in this paper

No.	Abbreviation	Description
1	Blk	Block additive with tuned proposal $N(\mathbf{0}, \lambda^2 \mathbf{I})$ .
2	MwG	Sequential additive with tuned proposals $N(\mathbf{0}, \lambda_i^2)$ ( $i = 1, \dots, 4$ ).
3	BlkShp	Block additive with tuned proposal $N(\mathbf{0}, \lambda^2 \hat{\Sigma})$ .
4	BlkShpCau	Block additive with tuned proposal Cauchy( $\mathbf{0}, \lambda^2 \hat{\Sigma}$ ).
5	BlkShpMul	Block multiplicative with tuned proposal $N(\mathbf{0}, \lambda^2 \hat{\Sigma})$ .
6	BlkAdpMul	Block multiplicative with adaptively tuned mixture proposal.
7	MwGRep	Sequential multiplicative/additive Gaussian; reparameterization.
8	MwGRepCau	Sequential multiplicative Gaussian and additive Cauchy; reparameterization.
9	IndShp	Block independence sampler with tuned proposal $t_5(0, \hat{\Sigma})$ .
10	Gibbs	Hidden data Gibbs sampler of Fearnhead and Sherlock (2006).

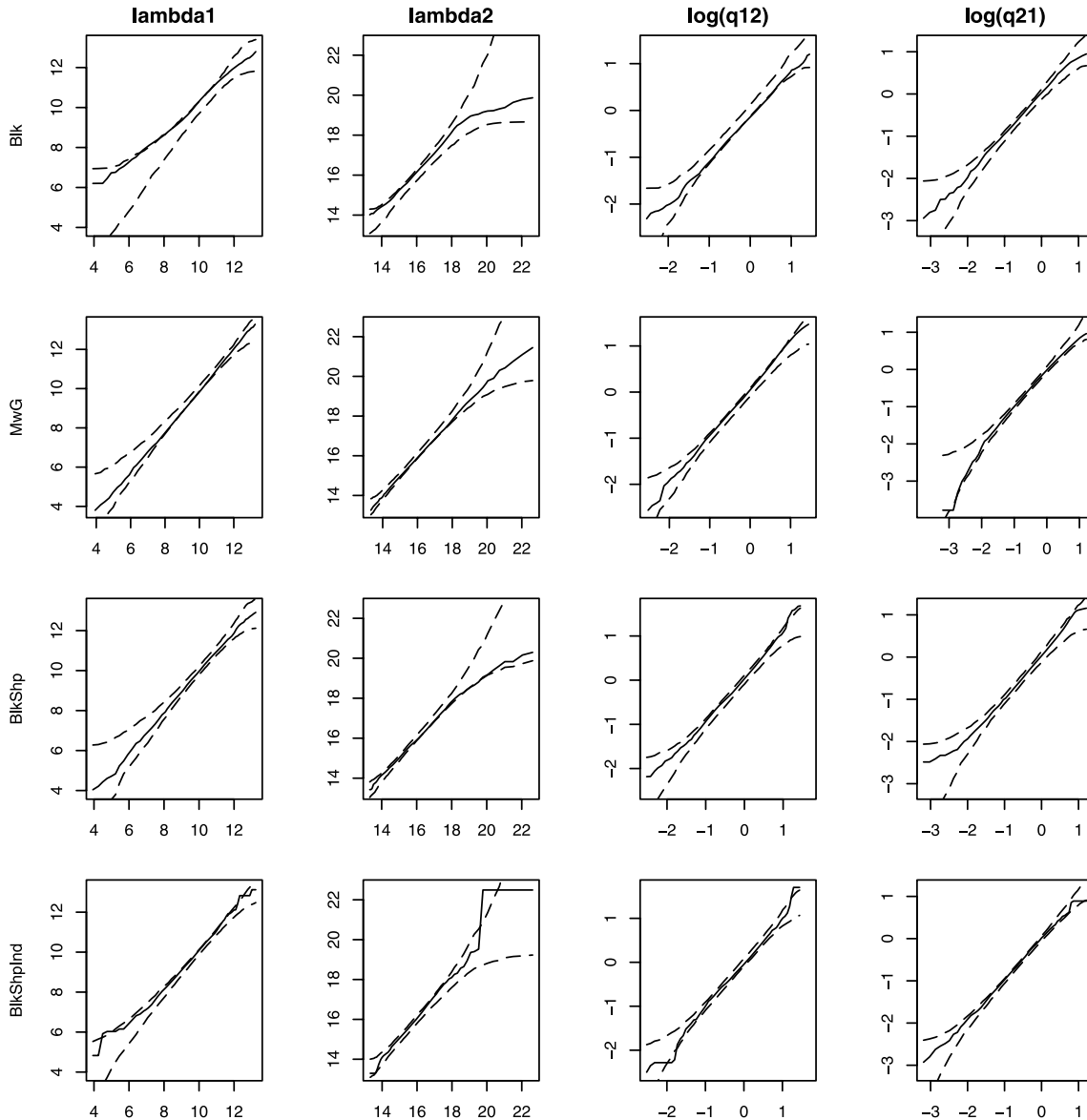


FIG. 4. *QQ plots for algorithms Blk, MwG, BlkShp, and IndShp, on D2 (Replicate 1). Dashed lines are approximate 95% confidence limits obtained by repeated sampling from iterations 1000 to 100,000 of a Gibbs sampler run; sample sizes were 10,000/ACT, which is the effective sample size of the data being compared to the Gibbs run.*

ations from that replicate. Calculation of the likelihood is by far the most computationally intensive operation (taking approximately 99.8% of the total CPU time) and is performed four times for each Metropolis-within-Gibbs-iteration (once for each parameter) and only once for each block update; a similar calculation is performed once for each update of the Gibbs sampler. To give a truer indication of overall efficiency the ACTs for each Metropolis-within-Gibbs replicate have therefore been multiplied by 4. Table 2 shows the mean adjusted ACT for each algorithm, parameter, and dataset. For each set of three replicates most of the ACTs lay

within 20% of their mean, and for the exceptions (Blk and BlkShpCau for datasets D1 and D2, and BlkShp and BlkShpMul for dataset D2) full sets of ACTs are given in Table 3 in the Appendix.

In general all algorithms performed better on D1 than on D2 because, as discussed in Section 2.3.1, dataset D1 contains more information on the parameters than D2; it therefore has lighter tails and is more easily explored by the chain.

The simple block additive algorithm using Gaussian proposals with variance matrix proportional to the identity matrix (Blk) performs relatively poorly on

TABLE 2

Mean estimated integrated autocorrelation time for the four parameters over three independent replicates for datasets D1 and D2

Algorithm	D1				D2			
	$\psi_1$	$\psi_2$	$\log(q_{12})$	$\log(q_{21})$	$\psi_1$	$\psi_2$	$\log(q_{12})$	$\log(q_{21})$
Blk	66	126	15	19	176	175	80	70
MwG*	22	22	33	33	103	90	114	99
BlkShp	13	18	13	15	46	25	37	36
BlkShpCau	19	32	25	24	63	50	56	38
BlkShpMul	13	17	13	15	33	26	22	16
BlkAdpMul	12	12	14	14	20	20	17	23
MwGRep*	13	14	32	44	20	23	23	21
MwGRepCau*	14	15	37	42	24	233	25	23
IndShp <sup>+</sup>	3.7	5.5	3.5	3.7				
Gibbs	4.2	3.2	5.7	5.9	26	19	32	27

Notes: \*Estimates for MwG replicates have been multiplied by 4 to provide figures comparable with full block updates in terms of CPU time.  
<sup>+</sup>ACT results for the independence sampler for D2 are irrelevant since the MCMC sample was not an accurate representation of the posterior.

both datasets. In absolute terms there is much less uncertainty about the transition intensities  $q_{12}$  and  $q_{21}$  (both are close to 1) than in the Poisson intensities  $\psi_1$  (10) and  $\psi_2$  (17 for D1 and 30 for D2) since the variance of the output from a Poisson process is proportional to its value. The optimal single-scale parameter necessarily tunes to the smallest variance and hence explores  $q_{12}$  and  $q_{21}$  much more efficiently than  $\psi_1$  and  $\psi_2$ .

Overall performance improves enormously once block proposals are from a Gaussian with approximately the correct shape (BlkShp). The efficiency of the Metropolis-within-Gibbs algorithm with additive Gaussian updates (MwG) lies somewhere between the efficiencies of Blk and BlkShp but the improvement over Blk is larger for dataset D1 than for dataset D2. As discussed in Section 2.3.1 the parameters in D1 are more nearly independent than the parameters in D2. Thus for dataset D1 the principal axes of an elliptical approximation to the posterior are more nearly parallel to the cartesian axes. Metropolis-within-Gibbs updates are (by definition) parallel to each of the cartesian axes and so can make large updates almost directly along the major axis of the ellipse for dataset D1.

For the heavy-tailed posterior of dataset D2 we would expect block updates resulting from a Cauchy proposal (BlkShpCau) to be more efficient than those from a Gaussian proposal. However, for both datasets Cauchy proposals are slightly less efficient than Gaussian proposals. It is likely that the heaviness of the Cauchy tails leads to more proposals with at least one negative parameter, such proposals being automatically

rejected. Moreover,  $\hat{\Sigma}$  represents the main posterior mass, yet some large Cauchy jump proposals from this mass will be in the posterior tail. It may be that  $\hat{\Sigma}$  does not accurately represent the shape of the posterior tails.

Multiplicative updates (BlkShpMul) make little difference for D1, but for the relatively heavy-tailed D2 there is a definite improvement over BlkShp. The adaptive multiplicative algorithm (BlkAdpMul) is slightly more efficient still, since the estimated variance matrix and the overall scaling are refined throughout the run.

As was noted earlier in this section, due to our choice of exponential priors the quantities estimated in this article have exponential or lighter posterior tails and so all the nonadaptive algorithms in this article are geometrically ergodic. The theory in Section 3.4 suggests ways to improve tail exploration for polynomially ergodic algorithms and so, strictly speaking, need not apply here. However, the exponential decay only becomes dominant some distance from the posterior mass, especially for dataset D2. Polynomially increasing terms in the likelihood ensure that initial decay is slower than exponential, and that the multiplicative random walk is therefore more efficient than the additive random walk.

The adaptive overall scaling  $m$  showed variability of  $O(0.1)$  over the first 1000 iterations after which time it quickly settled down to 1.2 for all three replicates on D1 and to 1.1 for all three replicates on D2. Both of these values are very close to the scaling of 1.19 that would be used for a four-dimensional update in the scheme of Roberts and Rosenthal (2010). The algorithm similarly learned very quickly about the variance

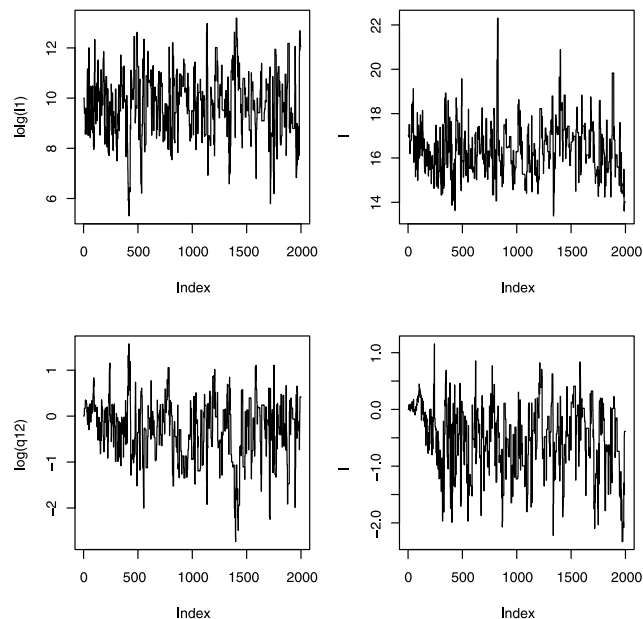


FIG. 5. Traceplots for the first 2000 iterations of BlkAdpMul on dataset D2 (Replicate 1).

matrix  $\Sigma$ , with individual terms settling down after less than 2000 iterations, and with exploration close to optimal after less than 500 iterations. This can be seen clearly in Figure 5 which shows traceplots for the first 2000 iterations of the first replicate of BlkAdpMul on D2.

The adaptive algorithm uses its own history to learn about  $d(d+1)/2$  covariance terms and a best overall scaling. One would therefore expect that the larger the number of parameters,  $d$ , the more iterations are required for the scheme to learn about all of the adaptive terms and hence reach a close to optimal efficiency. To test this a dataset (D3) was simulated from a three-dimensional MMPP with  $\psi = [10, 17, 30]^t$  and  $q_{12} = q_{13} = q_{21} = q_{23} = q_{31} = q_{32} = 0.5$ . The following adaptive algorithm was then run three times, each for 20,000 iterations.

**ALGORITHM 6B [BlkAdpMul(b)].** This adaptive algorithm is identical to BlkAdpMul (with  $d = 9$ ) except that no adaptive proposals were used until at least 100 nonadaptive proposals had been accepted, and that if an adaptive proposal was accepted then the overall scaling was updated with  $m \leftarrow m + 3\Delta/i^{1/2}$  so that the equilibrium acceptance rate was approximately 0.25.

Figure 6 shows the evolution of four of the 46 adaptive parameters (Replicate 1). All parameters seem close to their optimal values after 10,000 iterations, although covariance parameters appear to be still slowly

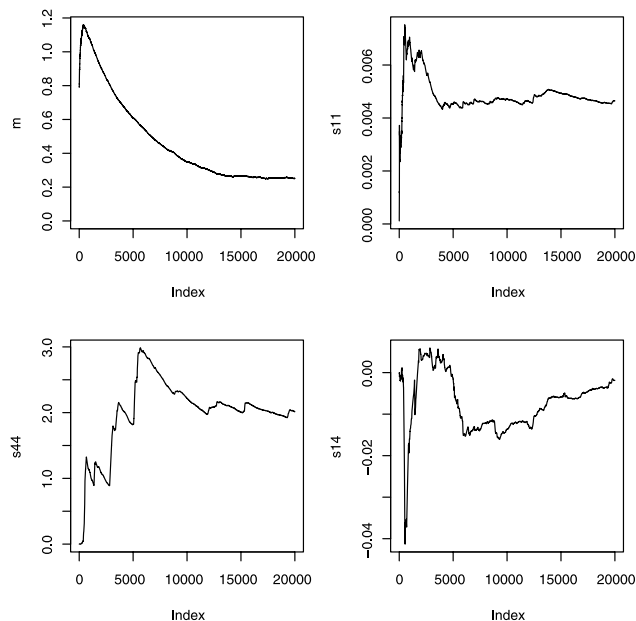


FIG. 6. Plots of the adaptive scaling parameter  $m$  and three estimated covariance parameters  $\text{Var}[\psi_1]$ ,  $\text{Var}[q_{12}]$ , and  $\text{Cov}[\psi_1, q_{12}]$  for BlkAdpMul(b) on dataset D3 (Replicate 1).

evolving even after 20,000 iterations. In contrast, traceplots of parameters (not shown) reveal that the speed of exploration of the posterior is close to its final optimum after only 1500 iterations. This behavior was repeated across the other two replicates, indicating that, as with the two-dimensional adaptive and nonadaptive runs, even a very rough approximation to the variance matrix improves efficiency considerably. Over the full 20,000 iterations, all three replicates showed a definite multimodality with  $\lambda_2$  often close to either  $\lambda_1$  or  $\lambda_3$ , indicating that the data might reasonably be explained by a two-dimensional MMPP. In all three replicates the optimal scaling settled between 0.25 and 0.3, noticeably lower than the Roberts and Rosenthal (2010) value of  $2.38/\sqrt{9}$ . With reference to Section 3.1 this is almost certainly due to the roughness inherent in a multimodal posterior.

The reparameterization of Section 3.5.2 was designed for datasets similar to D2, and on this dataset the resulting Metropolis-within-Gibbs algorithm (MwGRep) is at least as efficient as the adaptive multiplicative random walk. On dataset D1, however, exploration of  $q_{12}$  and  $q_{21}$  is arguably less efficient than for the Metropolis-within-Gibbs algorithm with the original parameter set. The lack of improvement when using a Cauchy proposal for  $\beta$  (MwGRepCau) suggests that this inefficiency is not due to poor exploration of the potentially heavy-tailed  $\beta$ . Further investigation in the



$(\bar{\psi}, q, \alpha, \beta)$  parameter space showed that for dataset D1 only  $q$  was explored efficiently; the posteriors of  $\bar{\psi}$  and  $\beta$  were strongly positively correlated ( $\rho \approx 0.8$ ), and both  $\bar{\psi}$  and  $\beta$  were strongly negatively correlated with  $\alpha$  ( $\rho \approx -0.65$ ). Posterior correlations were small  $|\rho| < 0.3$  for all parameters with dataset D2 and for all correlations involving  $q$  for dataset D1.

The optimal scaling for the one-dimensional additive Cauchy proposal in MwGRepCau was approximately two thirds of the optimal scaling for the one-dimensional additive Gaussian proposal in MwGRep. In four dimensions the ratio was approximately one half. These ratios allow the Cauchy proposals to produce similar numbers of small to medium sized jumps to the Gaussian proposals.

The independence sampler is arguably the most efficient of all of the algorithms considered for D1. However, as discussed earlier in this section, there are doubts about the accuracy of its exploration of D2. Mengersen and Tweedie (1996) showed that an independence sampler is uniformly ergodic if and only if the ratio of the proposal density to the target density is bounded below, and that one minus this ratio gives the geometric rate of convergence. To ensure the lower bound it is advisable to propose from a relatively heavy-tailed distribution, such as the  $t_5$  used here. The problem in this instance arises because dataset D2 could, just possibly, have been generated by a single Poisson process with intensity  $\psi \approx (\psi_1 + \psi_2)/2$ . The resulting minor mode (or, more precisely, ridge) is some distance from the center of the distribution, resulting in a low ratio of proposal and target densities.

The Gibbs sampler of Fearnhead and Sherlock (2006) is accurate, with its efficiency directly related to the amount of information about the hidden Markov chain that is available from the data (Sherlock, 2006). Thus for D1 the Gibbs sampler is more efficient than the best RWM algorithms, but this is not the case for D2.

## 5. DISCUSSION

We have described the theory and intuition behind a number of techniques for improving the efficiency of random walk Metropolis algorithms and tested these on two data sets generated from Markov modulated Poisson processes (MMPPs). Tests on these datasets also showed a sensibly implemented RWM to be at least as good as some of the other available MCMC algorithms. Some RWM implementations were uniformly successful at improving efficiency, while for others success depended on the shape and/or tails of the posterior. All of

the underlying concepts discussed here are quite general and easily applied to statistical models other than the MMPP.

Simple acceptance rate tuning to obtain the optimal overall variance term for a symmetric Gaussian proposal can increase efficiency by many orders of magnitude. However, with our datasets, even after such tuning, the RWM algorithm was very inefficient. The effectiveness of the sampling increased enormously once the shape of the posterior was taken into account by proposing from a Gaussian with variance proportional to an estimate of the posterior variance. For Algorithms 3, 4, and 5 the posterior variance was estimated through a short “training run”—the first 1000 iterations after burn in of Algorithm 1.

As expected, use of the “multiplicative random walk” (Algorithm 5), a random walk on the posterior of the logarithm of the parameters, improved efficiency most noticeably on the posterior with the heavier tails. However, contrary to expectation, even on the heavier tailed posterior an additive Cauchy proposal (Algorithm 4) was, if anything, less efficient than a Gaussian. Tuning of Cauchy proposals was also more time-consuming since simple acceptance rate criteria could not be used.

Algorithm 6 combined the successful strategies of optimal scaling, shape tuning, and transforming the data, to create a multiplicative random walk which learned the most efficient shape and scale parameters from its own history as it progressed. This adaptive scheme was easy to implement and was arguably the most efficient RWM for each of the datasets. A slight variant of this algorithm was used to explore the posterior of a three-dimensional MMPP, and showed that in higher dimensions such algorithms take longer to discover close to optimal values for the adaptive parameters. These runs also confirmed the finding for the two-dimensional MMPP that RWM efficiency improves enormously with knowledge of the posterior variance, even if this knowledge is only approximate. For a multimodal posterior such as that found for the three-dimensional MMPP it might be argued that a different variance matrix should be used for each mode. Such “regionally adaptive” algorithms present additional problems, such as the definition of the different regions, and are discussed further by Roberts and Rosenthal (2010).

Metropolis-within-Gibbs updates performed better when the parameters were close to orthogonal, at which point the algorithms were almost as efficient as an equivalent block updating algorithm with

TABLE 3

Estimated ACT for the four parameters, on three independent replicates for Blk and BlkShpCau on dataset D1 and Blk, BlkShp, BlkShpCau, and BlkShpMul on dataset D2

Algorithm	$\psi_1$	$\psi_2$	$\log(q_{12})$	$\log(q_{21})$
Blk (D1)	59, 64, 75	120, 155, 104	12, 15, 17	19, 21, 17
BlkShpCau (D1)	28, 16, 12	36, 29, 31	20, 20, 35	26, 23, 24
Blk (D2)	121, 259, 146	107, 262, 157	41, 139, 61	51, 110, 48
BlkShp (D2)	54, 51, 34	23, 24, 29	40, 45, 27	50, 35, 23
BlkShpCau (D2)	46, 51, 92	46, 57, 48	31, 42, 94	39, 41, 34
BlkShpMul (D2)	53, 24, 23	22, 33, 25	20, 23, 24	17, 18, 13

tuned shape matrix. The best Metropolis-within-Gibbs scheme for dataset D2 arose from a new reparameterization devised specifically for the two-dimensional MMPP with parameter orthogonality in mind. On D2 this performed nearly as well as the best scheme, the adaptive multiplicative random walk.

The adaptive schemes discussed here provide a significant step toward a goal of completely automated algorithms. However, as already discussed, for  $d$  model-parameters, a posterior variance matrix has  $O(d^2)$  components. Hence the length of any “training run” or of the adaptive “learning period” increases quickly with dimension. For high dimension it is therefore especially important to utilize to the full any problem-specific knowledge that is available so as to provide as efficient a starting algorithm as possible.

#### APPENDIX: RUNS WITH HIGHLY VARIABLE ACTS

Three replicates were performed for each dataset and algorithm, and ACTs are summarized by their mean in Table 2. However, for certain combinations of the algorithms and datasets the ACTs varied considerably; full sets of ACTs for these replicates are given in Table 3.

#### REFERENCES

- BAI, Y., ROBERTS, G. O. and ROSENTHAL, J. S. (2009). On the containment condition for adaptive Markov chain Monte Carlo algorithms. Preprint.
- Bédard, M. (2007). Weak convergence of Metropolis algorithms for non-i.i.d. target distributions. *Ann. Appl. Probab.* **17** 1222–1244. [MR2344305](#)
- Bédard, M. (2008). Optimal acceptance rates for Metropolis algorithms: Moving beyond 0.234. *Stochastic Process. Appl.* **118** 2198–2222. [MR2474348](#)
- BURZYKOWSKI, T., SZUBIAKOWSKI, J. and RYDEN, T. (2003). Analysis of photon count data from single-molecule fluorescence experiments. *Chem. Phys.* **288** 291–307.
- CARLIN, B. P. and LOUIS, T. A. (2009). *Bayesian Methods for Data Analysis*, 3rd ed. CRC Press, Boca Raton, FL. [MR2442364](#)
- DELLAPORTAS, P. and ROBERTS, G. O. (2003). An introduction to MCMC. In *Spatial Statistics and Computational Methods* (J. Moller, ed.). *Lecture Notes in Statistics* **173** 1–41. Springer, Berlin. [MR2001384](#)
- FEARNHEAD, P. and SHERLOCK, C. (2006). An exact Gibbs sampler for the Markov modulated Poisson processes. *J. R. Stat. Soc. Ser. B Stat. Methodol.* **68** 767–784. [MR2301294](#)
- GAMERMAN, D. and LOPES, H. F. (2006). *Markov Chain Monte Carlo*, 2nd ed. Chapman and Hall/CRC, Boca Raton, FL. [MR2260716](#)
- GEYER, C. J. (1992). Practical Markov chain Monte Carlo. *Statist. Sci.* **7** 473–483.
- GILKS, W. R., RICHARDSON, S. and SPIEGELHALTER, D. J. (1996). *Markov Chain Monte Carlo in Practice*. Chapman and Hall, London. [MR1397966](#)
- JARNER, S. F. and ROBERTS, G. O. (2002). Polynomial convergence rates of Markov chains. *Ann. Appl. Probab.* **12** 224–247. [MR1890063](#)
- KOU, S. C., XIE, X. S. and LIU, J. S. (2005). Bayesian analysis of single-molecule experimental data. *Appl. Statist.* **54** 1–28. [MR2137252](#)
- MENGERSEN, K. L. and TWEEDIE, R. L. (1996). Rates of convergence of the Hastings and Metropolis algorithms. *Ann. Statist.* **24** 101–121. [MR1389882](#)
- METROPOLIS, N., ROSENBLUTH, A. W., ROSENBLUTH, M. N., TELLER, A. H. and TELLER, E. (1953). Equations of state calculations by fast computing machine. *J. Chem. Phys.* **21** 1087–1091.
- MEYN, S. P. and TWEEDIE, R. L. (1993). *Markov Chains and Stochastic Stability*. Springer, London. [MR1287609](#)
- NEAL, P. and ROBERTS, G. (2006). Optimal scaling for partially updating MCMC algorithm. *Ann. Appl. Probab.* **16** 475–515. [MR2244423](#)
- ROBERTS, G. O. (2003). Linking theory and practice of MCMC. In *Highly Structured Stochastic Systems. Oxford Statist. Sci. Ser.* **27** 145–178. Oxford Univ. Press, Oxford. [MR2082409](#)
- ROBERTS, G. O. and ROSENTHAL, J. S. (2001). Optimal scaling for various Metropolis–Hastings algorithms. *Statist. Sci.* **16** 351–367. [MR1888450](#)
- ROBERTS, G. O. and ROSENTHAL, J. S. (2007). Coupling and ergodicity of adaptive Markov chain Monte Carlo algorithms. *J. Appl. Probab.* **44** 458–475. [MR2340211](#)

- ROBERTS, G. O. and ROSENTHAL, J. S. (2010). Examples of adaptive MCMC. *J. Comp. Graph. Stat.* **8** 349–367.
- ROBERTS, G. O., GELMAN, A. and GILKS, W. R. (1997). Weak convergence and optimal scaling of random walk Metropolis algorithms. *Ann. Appl. Probab.* **7** 110–120. [MR1428751](#)
- SCOTT, S. L. and SMYTH, P. (2003). The Markov modulated Poisson process and Markov Poisson cascade with applications to web traffic modelling. *Bayesian Statist.* **7** 1–10.
- SHERLOCK, C. (2005). In discussion of ‘Bayesian analysis of single-molecule experimental data.’ *J. Roy. Statist. Soc. Ser. C* **54** 500. [MR2137252](#)
- SHERLOCK, C. (2006). Methodology for inference on the Markov modulated Poisson process and theory for optimal scaling of the random walk Metropolis. Ph.D. thesis, Lancaster Univ. Available at <http://eprints.lancs.ac.uk/850/>.
- SHERLOCK, C. and ROBERTS, G. (2009). Optimal scaling of the random walk Metropolis on elliptically symmetric unimodal targets. *Bernoulli* **15** 774–798. [MR2555199](#)
- SOKAL, A. (1997). Monte Carlo methods in statistical mechanics: Foundations and new algorithms. In *Functional Integration (Cargèse, 1996)*. *NATO Adv. Sci. Inst. Ser. B Phys.* **361** 131–192. Plenum, New York. [MR1477456](#)